Meson Cloud Signatures in Semi-Inclusive DIS from Polarized Nucleons

W. Melnitchouk[a], A.W. Thomas[b]

[a] Department of Physics, University of Maryland, College Park, MD 20742, USA
[b] Department of Physics and Mathematical Physics, University of Adelaide, 5005, Australia

Abstract: We investigate the possibility of identifying an explicit mesonic component of the nucleon wavefunction through measurements of polarized Δ^{++} and Λ fragments produced in deep-inelastic leptoproduction off polarized protons. The meson-exchange model predicts a high correlation between the polarizations of the produced baryon and the target proton, in marked contrast with the competing diquark fragmentation process.

1 Introduction

A number of recent experiments have suggested quite non-trivial symmetry breaking effects among the nucleon's quark distributions. The $\overline{u} - \overline{d}$ asymmetry, for example, has been established by the New Muon and NA51 Collaborations at CERN [1], an intuitive understanding of which is provided by a pionic cloud around the nucleon [2]. A non-perturbative kaon cloud, on the other hand, may also generate an asymmetry between the strange and antistrange quark distributions in the nucleon, which the CCFR Collaboration [3] has recently investigated, as well as a polarized strange quark distribution, which may contribute to the explanation of the observed violation of the Ellis-Jaffe sum rule [4].

While strongly suggesting that non-perturbative effects play an important role in nucleon DIS, the results of these experiments do not rule out mechanisms other than meson clouds as those responsible for the symmetry breaking in the quark distributions. Indeed, the evidence for the meson cloud picture is rather indirect, and it seems a formidable challenge to seek direct experimental confirmation of mesonic effects in inclusive DIS. The pertinent question to ask is whether pions or kaons leave any unique traces at all in other processes, which cannot be understood in terms of perturbative quark and gluon degrees of freedom alone.

We propose a series of experiments involving tagged structure functions in semi-inclusive DIS on polarized protons, in which the nucleon's meson cloud may in fact give rise to rather characteristic fragmentation distributions in comparison with the predictions of parton model hadronization [5]. These differences will be significantly enhanced when initial and final state polarization effects are included [6]. With the high luminosity beam, polarized internal targets and 4π detectors capable of capturing slow moving baryons, one should be able to perform this experiment at HERMES.

2 Kinematics of Target Fragmentation

We focus on semi-inclusive production of polarized Δ^{++} baryons from a polarized proton, $e\vec{p} \to e'\vec{\Delta}^{++}X^-$. Because the g_1 structure function of a pion is zero, an unpolarized electron beam will suffice for this purpose. The choice of the Δ^{++} for the final state baryon reduces the backgrounds that one would otherwise have to consider due to the decay of Δs themselves. Furthermore, the decay products of Δ^+ or Δ^0 would include neutral hadrons whose detection would be more difficult, thus increasing the overall experimental uncertainties. Studies of the spin dependence of the fragmentation process here will require the target proton polarization to be parallel to the photon direction, with the spin of the produced baryon quantized along its direction of motion. Experimentally, the polarization of the produced $\vec{\Delta}^{++}$ (for the spin projection $\pm 3/2$ and $\pm 1/2$ states) can be reconstructed from the angular distribution of its decay products (p and π^+). For the case of the K cloud, the relevant reaction to observe is $e\vec{p} \to e'\vec{\Lambda}X^+$. Determining the polarization of the Λ hyperon is considerably easier because the Λ is self-analyzing.

In order to separate cleanly the target and current fragmentation regions requires high values of Q^2. With a 30 GeV electron beam at HERMES one will probe the $0.05 \lesssim x \lesssim 0.1$ region, which is relevant for the pionic contribution, up to $Q^2 \sim 5$ GeV^2 and $W^2 = (P+q)^2 \lesssim 50$ GeV^2, where P and q are the target nucleon and photon four-momenta, respectively.

In the rest frame of the nucleon the produced baryons will typically be slow, with three-momentum given by:

$$|\mathbf{p}| \;=\; \frac{1}{2M}\sqrt{(M^2 + M_B^2 - t)^2 - 4M^2M_B^2}\;, \tag{1}$$

where M is the nucleon mass, M_B the produced baryon mass, and $t = -p_T^2/\zeta - (M_B^2 - M^2\zeta)(1-\zeta)/\zeta$ is the four-momentum transfer squared between the proton and baryon, with $\zeta = p\cdot q / P\cdot q$ the light-cone fraction of the target proton's momentum carried by the baryon. The slowest baryons will be those for which t is maximized, which occurs when $\zeta \to 1$. As the upper limit on ζ is $1-x$, slow baryon production also corresponds to the $x \to 0$ limit, and the slowest possible particles produced at $\zeta = 1$ (at $x = 0$) will have momentum $|\mathbf{p}_{min}| = (M_B^2 - M^2)/2M \approx 340$ MeV for $B = \Delta$, and ≈ 193 MeV for $B = \Lambda$. For the pion-exchange process considered here, the peak in the differential cross section occurs at $|\mathbf{p}| \sim 600$ MeV, which, for $\zeta \sim 0.8$, corresponds to a missing mass of $p_X^2 = (P - p + q)^2 \sim 5$ GeV^2 for $Q^2 \sim 4$ GeV^2 at HERMES energies.

3 Pion Cloud Dynamics

The pion model is a dynamical model of the nucleon where the dissociation of a physical nucleon into a pion and an "undressed" nucleon or Δ is explicitly witnessed by the probing photon. In the pion-exchange model the differential cross section is:

$$\frac{d^5\sigma}{dx dQ^2 d\zeta dp_T^2} \;\propto\; \frac{\mathcal{F}^2_{\pi\Delta}(p_T^2,\zeta)\; F_2^\pi(x/(1-\zeta), Q^2)}{(t - m_\pi^2)^2}\mathcal{T}^{S\;s}(t), \tag{2}$$

where $\mathcal{F}_{\pi\Delta}$ is the hadronic pion–nucleon form factor, and F_2^π the pion structure function. The quantity $T^{S\;s}(t)$ is the amplitude for a nucleon of spin S to emit a pion of four-momentum squared t, leaving a Δ with spin s.

Note that Eq.(2) is correct only on the light-cone — in the instant-form approach the factorization of the γN cross section into $\gamma\ \pi$ and $\pi\ N$ cross sections holds only in the infinite momentum frame [7]. The formulation on the light-cone also allows one to use the on-mass-shell structure function of the pion in Eq.(2) [8], without the need to extrapolate the pion structure function into the (unknown) off-mass-shell region. For the $\pi N\Delta$ form factor in Eq.(2) we take the form suggested in earlier studies of the pionic content of the proton in inclusive DIS [8]:

$$\mathcal{F}_{\pi\Delta}(p_T^2,\zeta) \;=\; \left(\frac{\Lambda^2+M^2}{\Lambda^2+s_{\pi\Delta}}\right)^2, \tag{3}$$

where $s_{\pi\Delta} = (m_\pi^2+p_T^2)/(1-\zeta) + (M_\Delta^2+p_T^2)/\zeta$. Since the form factor on the light-cone is not yet very well constrained, other forms for its shape are also possible, however the effects discussed will be largely insensitive to the form factor details, and will be dictated entirely by the proton–pion spin correlations.

Because it is emitted collinearly with the pion, production of Δ baryons with helicity $\pm 3/2$ is forbidden, which leads to the selection rule:

$$\mathcal{T}^{S\ \pm\frac{3}{2}}(t) \;=\; 0. \tag{4}$$

The yield of spin projection $\pm 1/2$ states is finite, on the other hand, and given by:

$$\mathcal{T}^{+\frac{1}{2}\ \pm\frac{1}{2}}(t) \;=\; \frac{1}{12M_\Delta^2}\left[(M-M_\Delta)^2-t\right]\ \left[(M+M_\Delta)^2-t\right]^2\ (1\pm\cos\alpha). \tag{5}$$

Because the production of Δ baryons is limited to forward angles in the target rest frame, the factor $(1\pm\cos\alpha)$ associated with the final state polarization will significantly suppress the $s=-1/2$ yield relative to that of $s=+1/2$ final states.

The differential cross section, $Q^2d^3\sigma/dxdQ^2d\zeta$, for the individual polarization states of the produced Δ^{++} (for DIS from a proton with $S=+1/2$) is shown in Fig.1(a) for typical HERMES kinematics, $x=0.075$, $Q^2=4$ GeV^2 and $E=30$ GeV. The pion-exchange model predictions (solid curves) use the form factor in Eq.(3) with a cut-off $\Lambda=800$ MeV, which is consistent with the earlier studies of the contribution of the pion cloud to the inclusive cross sections [8], and which gives for the average number density of the $\pi\Delta$ component $< n >_{\pi\Delta}\approx 0.02$. The spectrum shows strong correlations between the polarizations of the target proton ($S=+1/2$) and the Δ^{++}.

A potentially significant background will be that due to uncorrelated spectator fragmentation. We can estimate the importance of this process within the parton model framework, in which the differential cross section is assumed to factorize into a product of the polarized quark distribution in the nucleon with the fragmentation function for the spectator system to fragment into a baryon with polarization s. For the quark helicity distributions we can use the parametrization from Ref.[9], while for the fragmentation functions we adopt the model of Ref.[6], which combines empirical [10] information on the unpolarized diquark fragmentation functions together with SU(6) relations amongst the spin-dependent fragmentation functions.

In Fig.1(a) the parton model predictions (dashed) for the various polarization states of the Δ are plotted in comparison with the pion-exchange cross sections. In the quark-parton model the correlations are significantly weaker, with the ratio of polarized Δs being $s=+3/2:+1/2:-1/2:-3/2\approx 3:2:1:0$. The comparisons assume that there is no significant interference

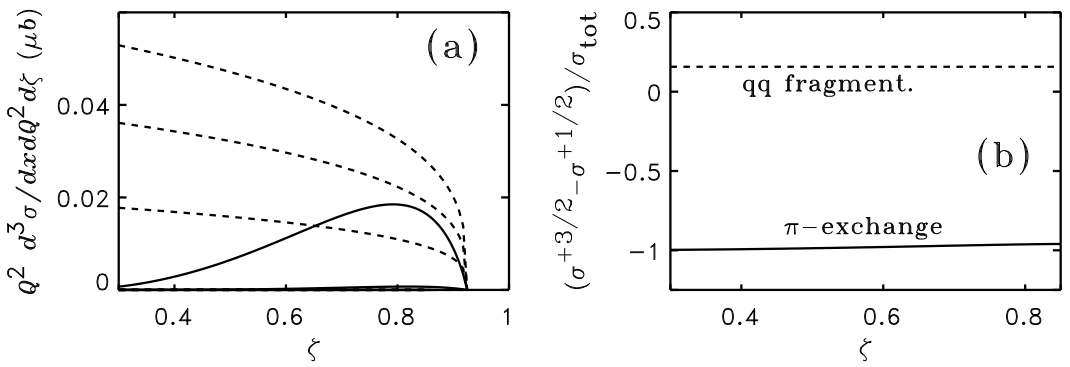

Figure 1: (a) *Differential electroproduction cross section for various polarization states of the* Δ^{++} *(for* $x = 0.075$*,* $Q^2 = 4\ GeV^2$ *and* $E = 30\ GeV$*). The* π*-exchange model predictions (solid curves: top* $s = +1/2$*, bottom* $s = -1/2$*) are for a cut-off mass* $\Lambda = 800\ MeV$*. The quark-parton model background estimates (dashed) are for* $s = +3/2$ *(largest),* $+1/2$ *and* $-1/2$ *(smallest).* (b) *Polarization asymmetry for the* π*-exchange (solid) and diquark (qq) fragmentation (dashed) models, where* $\sigma_{\rm tot}$ *is the sum over all polarization states.*

between the parton fragmentation and pion-exchange contributions. At small values of the exchanged four-momentum squared t one may expect this to be a good approximation, since the distance scales at which the pion and diquark are formed are rather different. For larger values of t this approximation may be less justifiable, and the possibility would exist that interference effects could modify the above simple predictions. This problem would be most pronounced for hard $\pi N\Delta$ vertices, however for relatively soft form factors ($\Lambda \lesssim 800$ MeV), as we have used, the above predictions should be a reliable guide.

Although the total unpolarized parton model cross sections are larger than the pion-exchange cross sections, even at larger values of ζ where the pionic effects are strongest, the differences between the pion-exchange model and fragmentation backgrounds can be enhanced by examining polarization asymmetries. Note that from the angular distributions of the decay $\Delta^{++} \to p\pi^+$ one will be able to experimentally differentiate the $s = \pm 3/2$ and $s = \pm 1/2$ components of the Δ. In Fig.1(b) we show the difference $\sigma^{+3/2} - \sigma^{+1/2}$, where $\sigma^s \equiv Q^2 d^3\sigma^{(s)}/dxdQ^2d\zeta$, as a fraction of the total unpolarized cross section. The resulting ζ distributions are almost flat, but significantly different for the two models. In particular, because of the selection rule in Eq.(4) the pion model predicts a large *negative* asymmetry, while the asymmetry in the diquark fragmentation model is small and *positive*. The ratios for t-dependent monopole and dipole form factors [8, 11], are almost indistinguishable from those in Fig.1(b). Therefore, a measurement of the polarization asymmetry appears to test only the presence of a pionic component of the nucleon wave function, independent of the details of the form factor.

Of course the two curves in Fig.1(b) represent extreme cases, in which Δs are produced entirely via pion emission or diquark fragmentation. In reality we can expect a ratio of polarization cross sections which is some average of the curves in Fig.1(b). The amount of deviation from the parton model curve will indicate the extent to which the pion-exchange process contributes. Unlike inclusive DIS, which can only be used to place upper bounds on the pion number, the semi-inclusive measurements could pin down the absolute value of $< n >_{\pi\Delta}$.

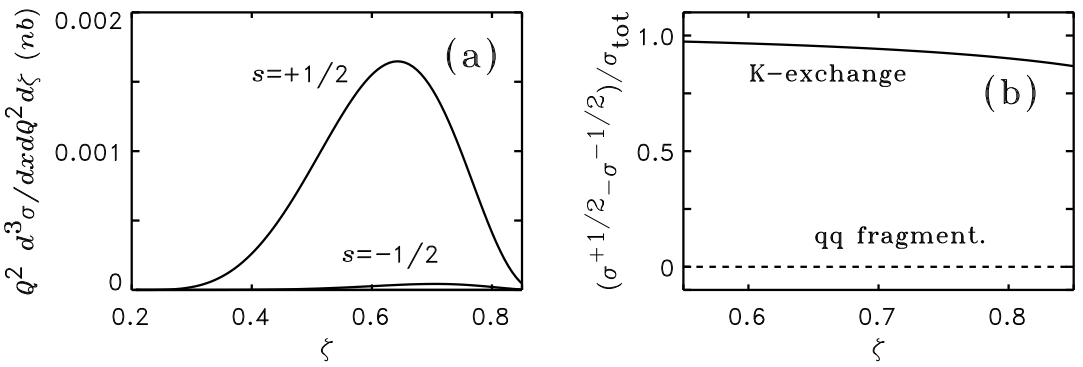

Figure 2: (a) Λ *production cross section in the* K*-exchange model, for a form factor cut-off* $\Lambda = 800$ *MeV, for* $s = +1/2$ *(upper solid curve) and* $s = -1/2$ *(lower solid) final states.* (b) *Polarization asymmetry for* K*-exchange (solid) compared with a leading fragmentation approximation estimate for the parton fragmentation process (dashed). (The kinematic conditions are as in Fig.1.)*

4 Kaon Cloud of the Nucleon

A direct test of the presence of a kaon cloud of the nucleon would be to observe also the differential Λ production cross section at large ζ, and in particular the relative polarization yields. Although some data do exist for Λ production in the target fragmentation region [12], the large errors and limited kinematical range covered do not permit one to unambiguously discern the presence of K effects.

The differential hyperon H $(= \Lambda, \Sigma^0)$ production cross section (included in the observed Λ cross section will be contributions from Σ^0 recoil states, which subsequently decay to $\Lambda\gamma$) is similar to the pion cross section in Eq.(2), with the trace factor here given by:

$$\mathcal{T}_H^{+\frac{1}{2}\ \pm\frac{1}{2}}(t) \ = \ \frac{1}{2}\Big((M_H - M)^2 - t\Big)\,(1 \pm \cos\alpha)\,, \tag{6}$$

for a proton initially polarized in the positive-z direction.

The Λ production cross section for the two possible polarizations in the K-exchange model, with a form factor cut-off $\Lambda = 0.8$ GeV, is shown in Fig.2(a) as a function of ζ. The target and recoil polarizations are predicted to be very strongly correlated, so that the asymmetry shown in Fig.2(b) for the cross sections $(\sigma^{+1/2} - \sigma^{-1/2})/(\sigma^{+1/2} + \sigma^{-1/2})$ is almost unity. The K-exchange ratios are very similar to the π-exchange results in Fig.1(b), indicating the similar spin transfer dynamics inherent in the meson cloud picture of the nucleon.

This is in strong contrast with the expectation from the $qq \to \Lambda$ diquark fragmentation picture, in which the target–recoil spin correlation is much weaker. In fact, to a first approximation the $\Lambda^{\uparrow\downarrow}$ yields in the quark-parton model are equal [6]. Since one has equal probabilities to form a $\Lambda^{\uparrow}$ and $\Lambda^{\downarrow}$, in the leading fragmentation approximation the asymmetry will be zero. Of course, SU(6) symmetry breaking effects, as well as non-leading fragmentation contributions, will modify this result, as will contributions from the production and decay of $\Sigma^{0\uparrow\downarrow}$ hyperons. However, the qualitative result that the asymmetry is small should remain true. Therefore the observation of a large polarization asymmetry in the large-ζ region of the target fragmentation region will be evidence for a kaon-exchange fragmentation mechanism.

5 Conclusion

We have outlined a series of semi-inclusive experiments on polarized proton targets that may for the first time enable one to unambiguously establish the presence of a pion and kaon cloud of the nucleon at high energies. Instrumental in identifying the mesonic signature will be detection of the polarization of the slow fragments in the target fragmentation region, which should largely eliminate the backgrounds resulting from the competing diquark fragmentation process. While the experiments proposed here are difficult, requiring all the intensity and duty factor one can obtain at HERMES, it does seem that they will provide quite clear information on the role of the pseudoscalar mesons in the nucleon.

References

[1] P.Amaudruz et al., Phys.Rev.Lett. **66** (1991) 2712; A.Baldit et al., Phys.Lett. B **332** (1994) 244.

[2] A.W.Thomas, Phys.Lett. **126** B (1983) 97.

[3] A.O.Bazarko et al., Z.Phys. C **65** (1995) 189.

[4] J.Ashman et al., Phys.Lett. B **206** (1988) 364.

[5] W.Melnitchouk and A.W.Thomas, in: Proceedings of the Workshop on CEBAF at Higher Energies, eds. N.Isgur and P.Stoler (April 1994) p.359.

[6] W.Melnitchouk and A.W.Thomas, Z.Phys. A **353** (1995) 311.

[7] W.Melnitchouk, A.W.Schreiber and A.W.Thomas, Phys.Rev. D **49** (1994) 1183.

[8] W.Melnitchouk and A.W.Thomas, Phys.Rev. D **47** (1993) 3794; A.W.Thomas and W.Melnitchouk, in: Proceedings of the JSPS-INS Spring School (Shimoda, Japan), (World Scientific, Singapore, 1993).

[9] T.Gehrmann and W.J.Stirling, Z.Phys. C **65** (1995) 461.

[10] M.Arneodo et al., Nucl.Phys. **B264** (1986) 739.

[11] L.L.Frankfurt, L.Mankiewicz and M.I.Strikman, Z.Phys. A **334** (1989) 343; E.M.Henley and G.A.Miller, Phys.Lett. B **251** (1990) 497; A.I.Signal, A.W.Schreiber and A.W.Thomas, Mod.Phys.Lett. A **6** (1991) 271; W.Melnitchouk, A.W.Thomas and A.I.Signal, Z.Phys. A **340** (1991) 85; S.Kumano and J.T.Londergan, Phys.Rev. D **44** (1991) 717; W.-Y.P.Hwang, J.Speth and G.E.Brown, Z.Phys. A **339** (1991) 383.

[12] M.Arneodo et al., Phys.Lett. **145** B (1984) 156.